

# Numerical methodology for analyzing the performance of a solar updraft tower in various environmental conditions

Arkadiusz Brenk <sup>\*</sup>; Ziemowit Malecha <sup>†</sup>; Lukasz Tomkow <sup>‡</sup>

## Abstract

This paper investigates a simplified and fast numerical model of a solar updraft tower. The model applies a novel approach to the calculation of heat transfer from the outside environment to a collector in the tower. Complex calculations of heat transfer are replaced by a properly defined heat flux boundary condition - the value of which depends on the time of day and meteorological conditions. The model was validated by experimental results from a pilot plant in Manzanares, Spain. Calculations were performed in order to investigate the effects of the chimney's height and the density of the solar radiation. Both of these dependencies were found to be logarithmic. The requirements for a 250 kW plant in various locations with different meteorological conditions were analyzed.

**Keywords** : Solar updraft tower, meteorological conditions, OpenFOAM, heat transfer

## 1 Introduction

1440- The solar chimney power plant (SCPP), also known as a solar updraft tower (SUT), is a simple device that converts solar radiation into mechanical and electrical power. It consists of a chimney with a wind turbine at its base and a greenhouse - an array of solar air heaters. During the operation of the device, air is initially heated in the greenhouse, then sucked through the wind turbine and further up the chimney due to the stack effect. The major advantage of this device is its simplicity and robustness. They can be easily constructed, even in countries without access to high technology, using readily available materials. And they are able to provide power for an extended period of time with minimal maintenance. However, conversion efficiency is very low, reported as 0.63% for a 5 MW plant [1].

<sup>\*</sup>Wrocław University of Science and Technology, Department of Cryogenics and Aerospace Engineering, Wyb Wyspińskiego 27, 50-370 Wrocław, Poland, [arkadiusz.brenk@pwr.edu.pl](mailto:arkadiusz.brenk@pwr.edu.pl)

<sup>†</sup>Wrocław University of Science and Technology, Department of Cryogenics and Aerospace Engineering, Wyb Wyspińskiego 27, 50-370 Wrocław, Poland, [ziemowit.malecha@pwr.edu.pl](mailto:ziemowit.malecha@pwr.edu.pl)

<sup>‡</sup>CERN, Esplanade des Particules 1, 1211 Geneva 23, Switzerland, [lukasz.tomkow@cern.ch](mailto:lukasz.tomkow@cern.ch)

In this paper, a new numerical modelling technique is proposed. It is validated by experimental results obtained from the Manzanares plant in Spain. The plant's maximum registered power output was 41 kW. The radius of the collector was 122 m and the height of the chimney - 194.6 m [2]; [3]. It was constructed in 1982 and was in operation until 1989.

Previous investigations into the numerical modelling of solar chimneys were performed using both commercial and in-house codes. Cao et al. used TRNSYS to analyze the transient behavior of a solar chimney depending on different meteorological conditions [4]. Fasel et al. used in-house code to investigate the steady and unsteady flow of air in the chimney and observed the appearance of convection cells [5]. Some improvements to the standard design were proposed. Guo et al. optimized the pressure ratio of the turbine using ANSYS and found that installing adjustable blades would yield better results [6]. Koonrisuk investigated the application of a sloped collector and found that in certain configurations, this leads to lower entropy generation [7]. Gong et al. proposed coupling the solar chimney with an inverted U-type cooling tower to obtain a self-powering device for cleaning air [8].

In the paper [9] the authors performed numerical studies of an SCPP system with parameters based on the Spanish prototype. Their numerical model was based on Fluent software and included a radiation model and a solar load model. The authors performed calculations for a wide range of solar radiation intensity. Nevertheless, only one height of the tower was examined and the research gave no detailed comparison with experimental data. Among other informative results, it was shown that while collector efficiency can vary with meteorological conditions, it remains in the range of 0.34 – 0.47.

Zhou et al. developed a pilot experimental solar chimney thermal power generating equipment [10]. They presented power outputs in steady state for differing global solar radiation intensity, collector area and chimney height. The range of height analyzed in this paper was limited to 8 meters and misleadingly suggested that the relationship of increase in power is

linear or even quadratic with the chimney height.

The investigations described in [10] were developed further in [11], where the authors analyzed the influence of a much wider range of chimney heights on solar chimney performance. Their study was based on a zero-dimensional and empirically supported theoretical model. It was shown that there is an optimal height of the SUT for which maximum energy was produced.

The analysis performed in the current paper was conducted for a wide range of SUT heights as well, but was done using state of the art CFD analysis. One of the results obtained suggested a logarithmic dependence between height and power output, and confirmed the existence of an economically justified optimal height for given meteorological conditions.

Numerical models applied in [5]; [6] explicitly analyzed the entire area of the solar collector. In the proposed model, the complex calculations of heat transfer from the outer environment to the collector were replaced with a properly defined heat flux boundary condition. Its functionality was extended to make it dependent on time and weather conditions.

Next, a number of calculations were performed in order to investigate the effects of the chimney's height and the density of solar radiation on the performance of the solar tower. A mathematical formula was created to describe these dependencies. The proposed model was used to estimate requirements for a 250 kW solar tower plant in various locations with differing meteorological conditions.

## 2 Methods

The presented simulations were carried out using OpenFOAM (Open Source Field Operation and Manipulation) [12]; [13]. The robustness and trustworthiness of this open source software have been proven multiple times by the authors in diverse and challenging applications. Among these, the works [14]; [15]; [16] deal with nonstandard and highly complex fluid flow and heat transfer systems.

Numerical calculations were made using *buoyantPimpleFoam* solver available in OpenFOAM. It exploits finite volume discretization in conjunction with the PISO (Pressure Implicit with Splitting of Operators) algorithm for compressible flows [17]; [18]; [19]. PISO schemes form part of the family of pressure correction methods.

The vector field of flow velocity is found by solving the

Navier-Stokes equation for a compressible fluid [20]:

$$\frac{\partial \rho \mathbf{u}}{\partial t} + \nabla \cdot (\rho \mathbf{u} \mathbf{u}) = -\nabla p + \nabla \cdot (\mu \nabla \mathbf{u}) + \mathbf{g} \rho, \quad (1)$$

where  $\mathbf{u} = (u, v, w)$  is a velocity vector,  $\rho$  - fluid density,  $\mu$  - dynamic viscosity,  $\mathbf{g}$  - gravitational acceleration.

Conservation of mass is ensured by the continuity formula:

$$\frac{\partial \rho}{\partial t} + \nabla \cdot (\rho \mathbf{u}) = 0. \quad (2)$$

To find the density of air the ideal gas formula was applied:

$$\rho = \frac{1}{RT} p, \quad (3)$$

where  $R = 287 \text{ J}/(\text{Kg} \cdot \text{K})$  is the individual gas constant of air.

The air temperature was obtained from the energy equation:

$$\frac{\partial \rho h}{\partial t} + \nabla \cdot (\rho \mathbf{u} h) = \frac{Dp}{Dt} + \nabla \cdot \left( \frac{k}{C_p} \nabla h \right) \quad (4)$$

where  $k$  is thermal conductivity of air,  $C_p$  - heat capacity of air.

In the case of realistic meteorological conditions and SUT sizes, the flow in the SUT is expected to be highly turbulent [21]; [22]. In the present study the standard  $k - \epsilon$  model was used to simulate the unresolved turbulent scales. In the numerical mesh the viscous sub-layer was not resolved and the standard wall function was employed.

The numerically modelled solar tower has a similar geometric shape to the Manzanares facility. The initial analysis is performed in order to compare the results of the numerical calculations with experimental data. The height of the chimney in the model is  $h = 195 \text{ m}$  with radius of  $r_c = 5 \text{ m}$ . The tubular section of the chimney starts 12 m above ground level. The collector has the shape of a flattened cone with its top cut off. Its internal radius is 14 m and external is  $r = 122 \text{ m}$  and its height above the ground varies between 2.2 m next to the connection with the chimney and 1.5 m on the external edge.

The connection between the chimney and the collector is the fragment of an ellipse tangential to both surfaces. Part of the region at the bottom of the chimney is cut to model a nozzle. The general view

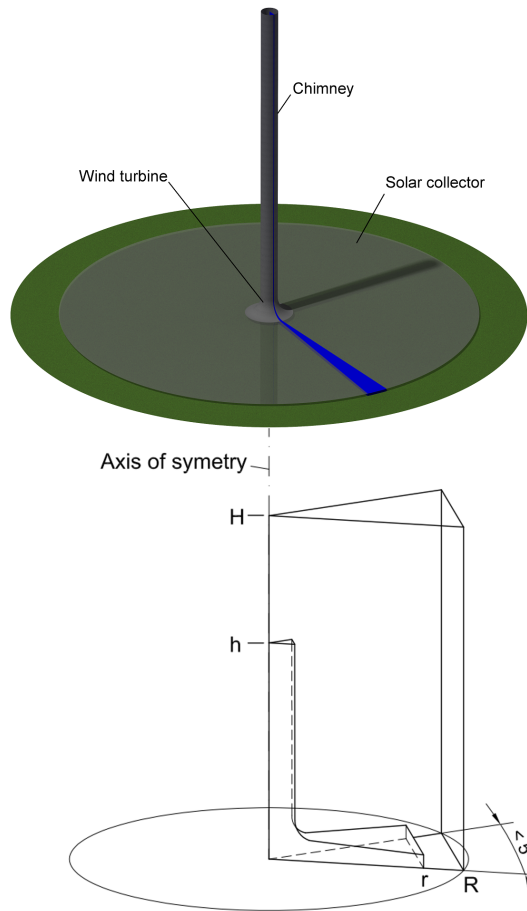


Figure 1: Upper: general view of the 3D original of the considered solar tower geometry with the modelled 2D wedge section marked in blue; Lower: 2D simplification of the 3D original geometry shown to the left. Notice that the 2D domain has a wedge shape and axial symmetry is assumed. The modeled solar tower and collector are submerged inside of a larger computational domain representing a fragment of an outside environment.

of the 3D original of the modelled system is presented on the picture on the left-hand side in figure 1.

One of the main challenges of the considered problem was the fact that it was both an external and an internal flow problem simultaneously. The flow in the collector and the tower was the internal flow problem, but the flow in the outside environment was the external flow problem.

The issue was resolved by placing the whole structure of the solar tower with the collector in a larger computational domain representing a fragment of the outside environment. In general, this methodology allows one to input an arbitrary intensity and direction of an ambient wind. In the current study, the primary focus was placed on the performance of the solar tower

itself and no outside wind was considered. Such analysis would be possible with the current model if minor adjustments were made.

The outside computational domain took the shape of a cylinder with height  $H$  and radius  $R$ . Consequently, the flow in the tower was established naturally rather than being forced by prescribing boundary conditions at an inlet and outlet from the tower. Accordingly, the walls of the tower and collector were modeled as inner obstacles placed in the computational domain and were modeled as zero-thickness thermal baffles with prescribed thermal conditions.

The size of the computational domain was chosen to minimize the influence of external boundary conditions on flow in the solar tower and to maximize computational efficiency. Finally its height was chosen to be  $H \sim 2.5h$  and radius  $R \sim 1.25r$ , see the right hand side picture in the figure 1.

The calculation speed of the model was increased substantially by taking advantage of the symmetry of the system and by optimizing the mesh. An axially symmetrical 2D hexahedral mesh was used and a single sector with a span smaller than  $5^\circ$  was modelled. In order to validate the 2D simplification, a diagnostic 2D model was successfully compared with its 3D original. The quality of the mesh was checked by mesh independence analysis.

The area of computational cells of the finest mesh considered in the independence analysis varied from  $0.0002 m^2$ , at the chimney's walls to  $6 m^2$  in the bulk of the domain (outside the chimney). The coarsest mesh, assuring statistically the same results as the finest mesh, had cell area in the range of  $0.003 m^2$ , at the walls to  $24 m^2$  in the bulk of the domain. In the presented numerical calculations, the computational mesh was built based on the cell sizes of the second mesh.

Symmetry (wedge) conditions were applied on the external boundaries in the angular direction (front and back of the domain) to maintain axial symmetry. On the top and side of the external domain constant temperature (depending on meteorological conditions) and zero gradient for pressure and velocity were prescribed. The ground and walls of the chimney were assumed to have zero gradient condition for temperature (no heat flux condition).

The energy deposited in the air below the collector was modeled as a heat flux condition prescribed on the collector's boundaries. Its value depended on the meteorological conditions and its definition is explained in detail below.

Previously applied numerical models explicitly analyzed the entire area of the solar collector [6]; [5]. In

the proposed model the complex calculations of heat transfer were replaced with the single parameter of heat transferred to the collector per unit volume ( $\dot{h}$ ). Additionally the  $\dot{h}$  parameter was made dependent on time, the meteorological conditions and the position of the Sun.

In order to account for different modes of heat transfer several assumptions were made. It was assumed that the roof of the collector was a single glass plate with the transmissivity of solar radiation equal to 0.85. 53% of the remaining energy was assumed to be absorbed by the ground, while the remaining part was accumulated in the volume of the collector and heated up the air. A Sankey diagram of the energy distribution is presented in figure 2.

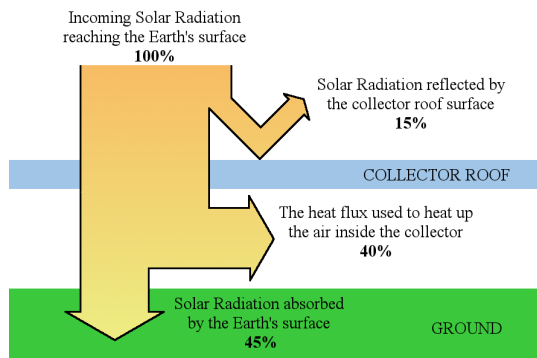


Figure 2: Distribution of solar energy arriving at the collector.

In order to find  $\dot{h}$ , the instantaneous flux of solar energy  $\dot{q}_s(t)$  given in  $W/m^2$  has to be considered. It is calculated based on the assumption of sinusoidal distribution of the solar energy during the day:

$$\dot{q}(t) = \begin{cases} \dot{q}_{av} \cdot (\sin(A) + 1), & t \in \langle 12 - \frac{t_d}{2} : 12 + \frac{t_d}{2} \rangle \\ 0, & t \notin \langle 12 - \frac{t_d}{2} : 12 + \frac{t_d}{2} \rangle \end{cases} \quad (5)$$

where  $A = \frac{(t - (12 - \frac{t_d}{2})) \cdot \pi \cdot 2}{t_d} - \frac{\pi}{2}$  and  $\dot{q}_{av}$  is the average daily insolation and  $t_d$  is the daily period of solar operation. Then  $\dot{h}$  is calculated with the following formula:

$$\dot{h}(t) = 0.4 \cdot \frac{\dot{q}(t) \cdot A_c}{V_c}, \quad (6)$$

The formula (6) takes into consideration the aforementioned losses,  $A_c$  is the area of the collector and  $V_c$  is the volume of air under it.

Figure 3 shows a comparison of the heat flux calculated using the formula (6) for the Manzanares location and its comparison with real meteorological data gathered at this location.

As mentioned earlier, the model that was developed assumed constant collector efficiency of 0.4. In general, collector efficiency can vary with the meteorological data, typically in the range of 0.34–0.47 [9]. Nevertheless, the satisfactory comparison of the presented results with the experimental data showed that the value of 0.4 was properly chosen and most likely, its constancy did not have a major influence on the results obtained. Moreover, it significantly simplified the model.

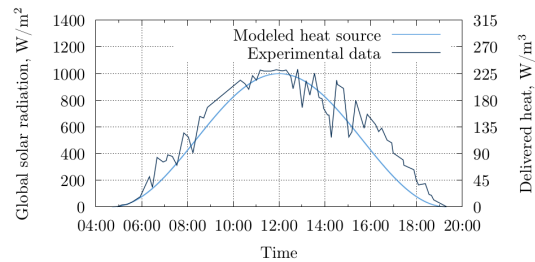


Figure 3: Comparison of the heat flux calculated using the formula (6) for the Manzanares location and its comparison with real meteorological data gathered at this location.

The simplification of the collector region enables faster computation while keeping the numerical results close to the experimental ones. Complex heat transfer relations are replaced with a properly defined boundary condition.

### 3 Results and Discussion

The comparison between the experimental and numerical results for the Manzanares solar tower is presented in the figure 4. The plots from the figure compare changes in power output as a function of the time of day. Satisfactory comparison can be seen and the proposed numerical model is validated.

The visible discrepancy for the time after 19:00 can be explained by a lack of implementation of a ground heat release mechanism after sunset. This mechanism was not crucial for the scope of the current studies, where the isolated influence of tower height and geographical location on solar tower performance are examined. The introduced numerical methodology could be independently expanded with this mechanism.

Figure 5 shows temperature and velocity magnitude distribution in the collector and along the chimney for the chimney's height of 300 m and the solar radiation of  $500 W/m^3$ . It should be noted that the direction of the velocity vector in the chimney is predominantly vertical and the velocity magnitude shown

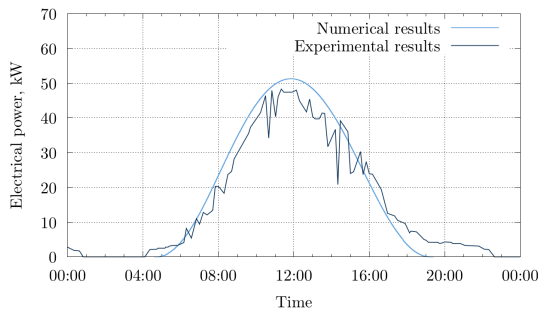


Figure 4: Comparison of the experimental data and numerical results of the Manzanares solar tower. Satisfactory comparison can be seen.

on the figure varies close to the vertical component of the velocity, compare with the figure 6a.

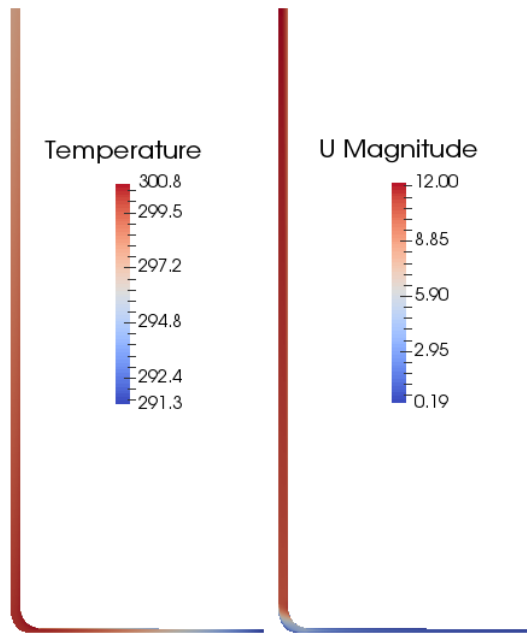


Figure 5: Temperature and velocity magnitude distribution along the SUT for chimney height of 300 m and solar radiation of  $500 \text{ W/m}^2$ . Note that for better visibility only the SUT is shown.

Figure 6a shows the flow velocities established in the chimney as a function of time and for various chimney heights  $h = (50, 75, 100, 150, 200, 300) \text{ m}$  for solar radiation  $500 \text{ W/m}^2$ . It can be noticed that steady flow was achieved for time  $\approx 600 \text{ s}$ . The steady-state velocities as a function of tower height are shown in figure 6b. It can be seen that this dependency is logarithmic in nature.

In the same manner, the dependence of flow velocity on the intensity of solar radiation was analyzed. Figure 7 shows temperature and velocity magnitude

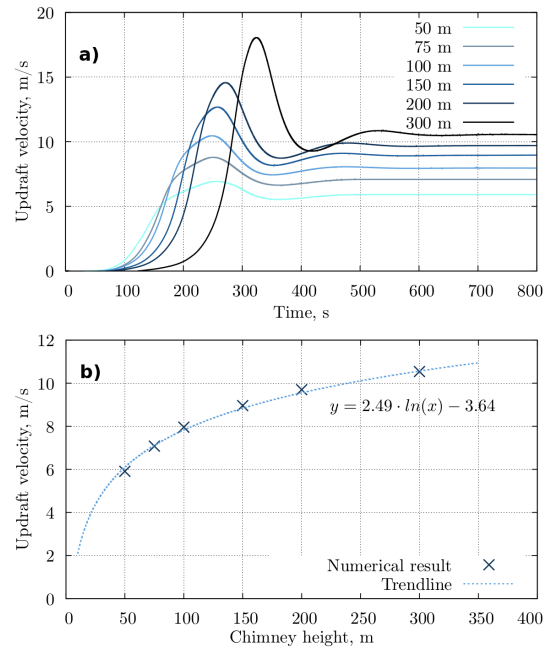


Figure 6: a) Changes of velocity in time in the solar tower for various chimney heights; b) Steady-state velocities established in the chimney as a function of chimney height.

distribution in the collector and along the chimney for the solar radiation of  $50 \text{ W/m}^3$  and  $250 \text{ W/m}^3$ . It should be noted that the direction of the velocity vector in the chimney is predominately vertical and the velocity magnitude shown on the figure is vary close to the vertical component of the velocity, compare with the figure 8a.

Figure 8a shows the dependence of the updraft flow velocity in time in a function of the solar radiation for the tower with geometry similar to Manzanares. The steady state results and the corresponding approximating function are presented in figure 8b. As in the previous case, it has the logarithmic nature.

The logarithmic form of both approximated functions shows that only an initial increase of the height of the tower can have a significant impact on the obtained power. It suggests an existence of an optimal tower high, above which the further increase of its height would not result in significant increase of the power. This observation, based on the presented comprehensive CFD analysis, reaffirms the conclusions stated in [11] and validates the 0D theoretical model proposed there.

Similarly, for a given tower height, only an initial increase of the intensity of solar radiation would significantly influence the obtained power. The further increase would not have such strong impact on power

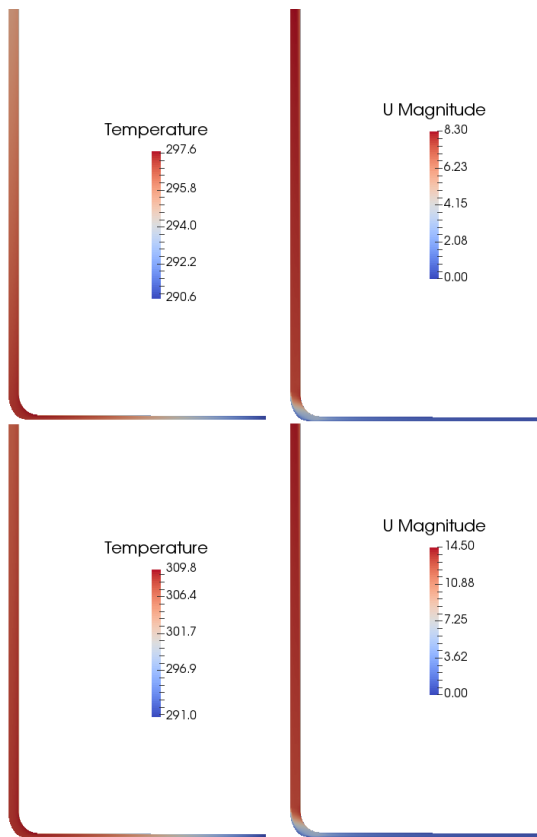


Figure 7: Upper(Lower) row: Temperature and velocity magnitude distribution along the SUT geometrically similar to Manzanares facility for the solar radiation of 50(250) $W/m^3$ .

generation any more.

Figure 10 shows the numerical results of an exemplary solar tower located in two different geographic regions: Poland and Sudan, characterized by a very distinct weather conditions presented in figure 9. It was assumed that the nominal power of the desired solar tower should reach 250 kW and was supplied with WES250 wind turbine with a rotor diameter of 30 m. The other dimensions of the analyzed solar tower are shown in table 1.

For simplicity, the physical model of the WES250 wind turbine was not coupled in the calculation. The turbine was coupled using its performance characteristic curve.

Figure 10a shows the dependence of flow velocity on the height of the tower for different radiation intensity conditions. The changes of power and velocity in function of day time are presented in figure 10b.

The numerical results show that the African location is much more favorable. To obtain the same velocity and power in Central European location the tower

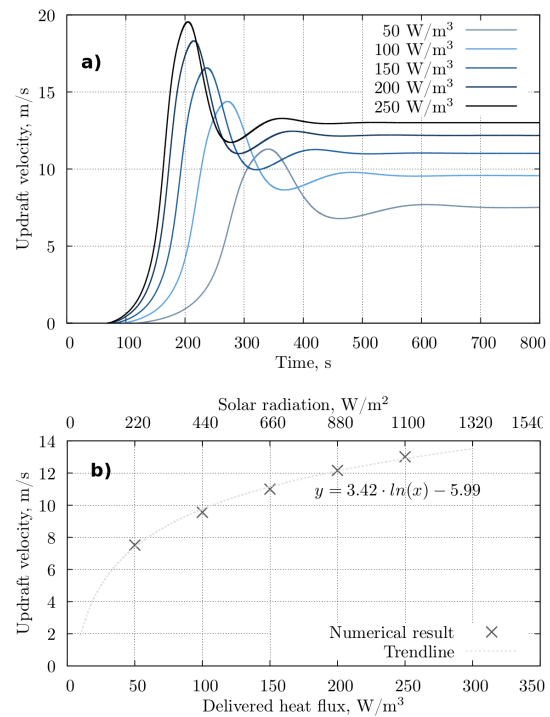


Figure 8: a) Changes of velocity in time in the solar tower for a various solar radiation intensity; b) Steady-state velocities established in the chimney in the function of the solar radiation intensity.

Table 1: Technical data of the proposed solar tower for numerical analysis.

Data	Value
Nominal installed power	250 kW
Wind turbine type	WES250
Chimney radius	15 m
Height of chimney beginning	20 m
Collector radius	35 to 250.0 m
Collector height	2 to 4 m
Collector area	192 510 m <sup>2</sup>
Volume under collector	536 794 m <sup>3</sup>
Radius of transition area	25 m

would have to be 3 times higher. Such design is unfeasible from engineering, financial and environmental point of view. The obtained power would be small when compared to other possible power sources using the same resources.

On the other hand, the construction and exploitation of the tower with the smaller height is relatively cheap and simple. Such solution is readily applicable in hot and sunny regions with low technical background. The analysis showed that the application of solar towers in such regions could easily provide some of electric power without the effort connected with the construction of supply lines and other infrastructure.

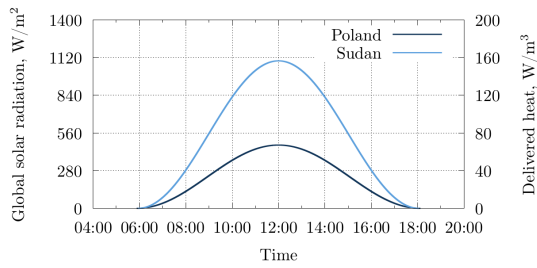


Figure 9: Solar radiation calculated using formula (6) for two different geographic regions: Poland and Sudan, characterized by a very distinct weather conditions.

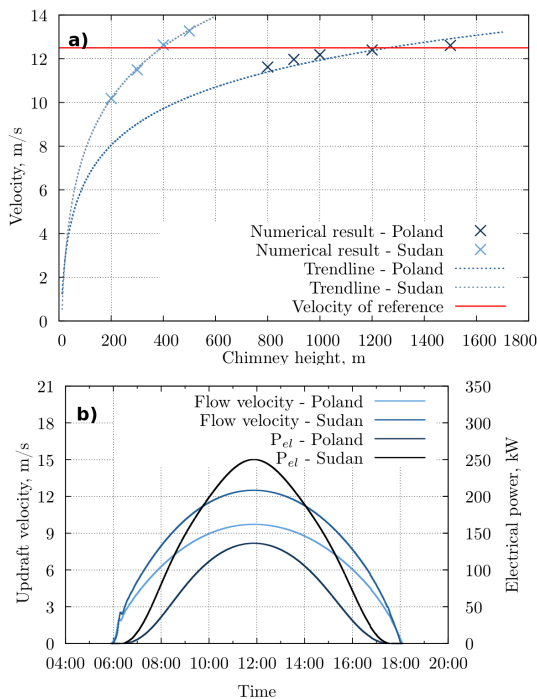


Figure 10: Comparison of numerical results obtained for exemplary locations characterized with distinct weather conditions; a) Changes of the updraft velocity in a function of the chimney height; b) Changes of the updraft velocities and corresponding power production in a function of the time of a day.

## 4 Conclusions

The presented numerical model proved to be fast and reliable. The presented numerical approach proposed to model a solar tower as a zero thickness thermal baffles located in a much larger computational domain representing a fragment of an outside environment. Thanks to that, the flow in the solar tower was established naturally as a response to the applied solar conditions, rather than being forced by defining boundary conditions at the inlet and outlet from the solar tower. The proposed 2D simplifications allowed for much faster calculations and gave opportunity to study a wide range of parameters, such as chimney’s height and solar intensity in reasonably short computational time. This methodology is ready to apply for solar towers with more complex, axial symmetric geometries, e.g. complex shape of the chimney. The proposed method for modeling of a heat delivery from the solar collector to the air, as a heat flux boundary condition greatly simplified the model. It allows for trustworthy numerical analysis of a solar tower operation in different regions with distinct meteorological conditions.

It was shown that the flow velocity in the chimney depends logarithmically on height and intensity of solar radiation. It has important consequences when comparing the feasibility of the technology in regions with different meteorological conditions.

## Acknowledgements

The work has been supported by statutory funds from Polish Ministry for Science and Higher Education for the year of 2018.

## References

1. Pasumathi, N., and Sherif, S.A. (1998) Experimental and theoretical performance of a demonstration solar chimney model Part I: mathematical model development. *International Journal of Energy Research*, **22** (3), 277288.
2. Haaf, W., Friedrich, K., Mayr, G., and Schlaich, J. (1983) Solar Chimneys Part I: Principle and Construction of the Pilot Plant in Manzanares. *International Journal of Solar Energy*, **2** (1), 320.
3. Haaf, W. (1984) Solar chimneys part II: preliminary test results from Manzanares Pilot Plant. *International Journal of Solar Energy*, **2** (2), 141161.

4. Cao, F., Li, H., Zhao, L., Bao, T., and Guo, L. (2013) Design and simulation of the solar chimney power plants with TRNSYS. *Solar Energy*, **98**, Part A, 2333.
5. Fasel, H.F., Meng, F., Shams, E., and Gross, A. (2013) CFD analysis for solar chimney power plants. *Solar Energy*, **98**, Part A, 1222.
6. Guo, P., Li, J., Wang, Y., and Liu, Y. (2013) Numerical analysis of the optimal turbine pressure drop ratio in a solar chimney power plant. *Solar Energy*, **98**, Part A, 4248.
7. Koonsrisuk, A. (2013) Comparison of conventional solar chimney power plants and sloped solar chimney power plants using second law analysis. *Solar Energy*, **98**, Part A, 7884.
8. Gong, T., Ming, T., Huang, X., Richter, R.K. de, Wu, Y., and Liu, W. (2017) Numerical analysis on a solar chimney with an inverted U-type cooling tower to mitigate urban air pollution. *Solar Energy*, **147**, 6882.
9. Guo, P., Li, J., Wang, Y., and Wang, Y. (2015) Numerical study on the performance of a solar chimney power plant. *Energy Conversion and Management*, **105**, 197205.
10. Zhou, X., Yang, J., Xiao, B., and Hou, G. (2007) Simulation of a pilot solar chimney thermal power generating equipment. *Renewable Energy*, **32** (10), 16371644.
11. Zhou, X., Yang, J., Xiao, B., Hou, G., and Xing, F. (2009) Analysis of chimney height for solar chimney power plant. *Applied Thermal Engineering*, **29** (1), 178185.
12. (2014) *The Open Source CFD Toolbox User Guide*.
13. Weller, H.G., Tabor, G., Jasak, H., and Fureby, C. (1998) A Tensorial Approach to Computational Continuum Mechanics Using Object-oriented Techniques. *Comput. Phys.*, **12** (6), 620631.
14. Bozza, G., Malecha, Z.M., and Weelderen, R.V. (2016) Development and application of a generic {CFD} toolkit covering the heat flows in combined solidliquid systems with emphasis on the thermal design of HiLumi superconducting magnets. *Cryogenics*, **80**, 253264.
15. Malecha, Z.M., Jedrusyna, A., Grabowski, M., Chorowski, M., and Weelderen, R. van (2016) Experimental and numerical investigation of the emergency helium release into the LHC tunnel. *Cryogenics*, **80**, 1732.
16. Chini, G., Malecha, Z., and Dreeben, T. (2014) Large-amplitude acoustic streaming. *J. Fluid Mech.*, **744**, 329351.
17. Ferziger, J.H., and Peric, M. (1999) *Computational Methods for Fluid Dynamics*, Springer, Berlin.
18. Issa, R.I., Gosman, A.D., and Watkins, A.P. (1986) The computation of compressible and incompressible recirculating flows by a non-iterative implicit scheme. *Journal of Computational Physics*, **62** (1), 6682.
19. Chung, T.J. (2002) *Computational Fluid Dynamics*, Cambridge University Press, Cambridge.
20. Batchelor G.K (2000) *An introduction to fluid dynamics*, Cambridge University Press.
21. Fasel, H.F., Meng, F., Shams, E., and Gross, A. (2013) CFD analysis for solar chimney power plants. *Solar Energy*, **98**, 1222.
22. Aurelio, M., and Bernardes, S. (2017) Preliminary stability analysis of the convective symmetric converging flow between two nearly parallel stationary disks similar to a Solar Updraft Power Plant collector. *Solar Energy*, **141**, 297302.
23. Fox, B (2014) *Wind power integration: connection and system operational aspects*, IET.
24. Kalogirou S.A (2013) *Solar energy engineering: processes and systems*, Academic Press.
25. (2003) *Grid convergence error analysis for mixed-order numerical schemes*.